


RESEARCH

Open Access



Lateral detrital C transfer across a *Spartina alterniflora* invaded estuarine wetland

Yu Gao^{1,2,3}, Jiquan Chen⁴, Tingting Zhang^{1,2}, Bin Zhao^{2*} , Steven McNulty⁵, Haiqiang Guo², Feng Zhao¹ and Ping Zhuang¹

Abstract

Background: The lateral movements of mass and energy across the terrestrial-aquatic interface are being increasingly recognized for their importance in the carbon (C) balance of coastal/estuarine wetlands. We quantified the lateral flux of detrital C in the Yangtze estuary where invasive *Spartina alterniflora* has substantially and extensively altered the ecosystem structure and functions. Our overall objective was to close the C budget of estuarine wetlands through field sampling, tower-based measurements, and modeling.

Methods: A lateral detrital C exchange evaluation platform was established in a case study of the Yangtze River Estuary to investigate the effect of ecosystem structural changes on lateral detrital C transfer processes. This study estimated the lateral detrital C exchange based on the gross primary production (GPP) by performing coupled modeling and field sampling. Tower-based measurements and MODIS time series and CH₄ outgassing and biomass simultaneously measured the lateral detrital C flux to characterize the relative contributions of lateral (i.e., detritus) C fluxes to the annual marsh C budget.

Results: The C pools in the plants and soil of *Spartina* marshes were significantly higher than those of the native community dominated by *Phragmites australis*. The GPP based on MODIS (GPP_{MODIS}) was 472.6 g C m⁻² year⁻¹ and accounted for 73.0% of the GPP estimated from eddy covariance towers (GPP_{EC}) (646.9 ± 70.7 g C m⁻² year⁻¹). We also detected a higher GPP_{MODIS} during the pre-growing season, which exhibited a similar lateral detrital C flux magnitude. On average, 25.8% of the net primary production (NPP), which ranged from 0.21 to 0.30 kg C m⁻² year⁻¹, was exported during lateral exchange. The annual C loss as CH₄ was estimated to be 17.9 ± 3.7 g C m⁻² year⁻¹, accounting for 2.8% of the GPP_{EC}. The net positive detrital C flux (i.e., more detritus leaving the wetlands), which could exceed 0.16 kg C m⁻² day⁻¹, was related to daily tides. However, the observed lateral detrital C flux based on monthly sampling was 73.5% higher than that based on daily sampling (i.e., the sum of daily sampling), particularly in March and October. In addition, spatiotemporal granularities were responsible for most of the uncertainty in the lateral detrital C exchange.

Conclusion: This research demonstrated that an integrated framework incorporating modeling and field sampling can quantitatively assess lateral detrital C transport processes across the terrestrial-aquatic interface in estuarine wetlands. However, we note some limitations in the application of the light-use efficiency model to tidal wetlands. *Spartina* invasion can turn the lateral C balance from a C source (209.0 g C m⁻² year⁻¹) of *Phragmites*-dominated marshes into a small C sink (-31.0 g C m⁻² year⁻¹). Sampling over a more extended period and continuous measurements

*Correspondence: zhaobin@fudan.edu.cn

² Ministry of Education Key Laboratory for Biodiversity Science and Ecological Engineering, Coastal Ecosystems Research Station of the Yangtze River Estuary, and Institute of Eco-Chongming (IEC), Fudan University, Shanghai 200438, China
Full list of author information is available at the end of the article

are essential for determining the contribution of different lateral detrital C flux processes to closing the ecosystem C budgets. The sampling spatiotemporal granularities can be key to assessing lateral detrital C transfer.

Keywords: Estuarine wetland, Carbon outwelling, Lateral carbon flux, Methane emission, *Spartina alterniflora*, *Phragmites australis*

Introduction

Mass and energy exchanges across the terrestrial-aquatic interface (e.g., riparian zones of streams, rivers, lakes, and coastal areas) have been increasingly examined over the last two decades, mainly through scientific investigations of the carbon (C) cycle and global change (Aufdenkampe et al. 2011; Cole et al. 2007; Harishma et al. 2020; Jenerette and Lal 2005; Tank et al. 2018). In land-sea interfaces, the lateral transports of mass and energy, in particular, have been recognized for their roles in ecosystem performances such as primary production (Aguios et al. 2020; Prasad et al. 2017; Rogers et al. 2019). Additionally, accurate estimates of lateral C exchange between tidal wetlands and adjacent estuarine waters are extremely valuable for testing outwelling ecological processes and developing adaptive management plans for these sensitive areas (Bouchard 2007; Odum 2000). Previous research has included measuring ecosystem production in coastal wetlands in the Yangtze River Estuarine area, direct measurements from eddy-covariance (EC) towers, and indirect estimates from remote sensing imagery. However, the mechanisms and consequences of uncertainty for estimating and observing lateral fluxes depend on the spatial (e.g., plot to landscape) and temporal (e.g., day—years) scales. These scale-dependent dynamics make closing C budgets more challenging (Duarte et al. 2017; Taillardat et al. 2019).

Regrettably, scientists have not yet reached a consistent conclusion regarding the percentage of C transported by tides, which possibly indicates site-specificity (Call et al. 2019; Huang et al. 2020). For example, at the landscape scale, one study showed that 45% of salt marsh primary production was transported into a nearby ocean by tidal movements over a year (Teal 1962). Additionally, much scientific interest has also focused on C outwelling at a bimonthly scale, and 12% of aboveground detritus is exported out of a low marsh (Palomo and Niell 2009). Similarly, it has been reported that approximately 14% of dead organic matter is washed away by tides at a monthly scale (Bouchard et al. 1998). However, other studies have found that tides might remove only 1% of salt marsh primary production in the form of litter on a daily scale (Dankers et al. 1984). These differences in lateral flows depend on the size of tides, the extent of the salt marsh, and the level of ecosystem productivity (Duarte et al. 2014), which make it highly challenging to capture the

actual coastal detritus input/output processes (Holden et al. 2012). This process is even more complicated when hydrologic flow paths are structured through tidal creeks that are highly variable over time and across coastal landscapes. A significant task is needed to integrate these hydrologic movements with improved methods to quantify, unify, and synthesize the available data (Gounand et al. 2018). There appear to be at least two immediate questions associated with the lack of C closure: How do lateral fluxes deviate from the C budget (i.e., CO₂, CH₄) through tidal activity? How much variation is due to the daily and monthly tidal movements? In addition to high temporal variations, spatial differences due to the vegetation type and structure, hydrological pathways (i.e., tidal creek), and landform can affect the lateral fluxes at terrestrial-aquatic interfaces (Najjar et al. 2018). Current estimates in the literature show substantial differences and even contradictions depending on the study site and season (Schindler and Smits 2017). In particular, the unknown fractionation of CH₄ highlights the challenge of accounting for elements that rapidly change in their C form. Additionally, we previously found that tower-based GPP (gross primary production) estimates are consistently and significantly higher than those obtained using MODIS (Moderate Resolution Imaging Spectrometer) (Gao et al. 2018). GPP differences of 53.4–65.0% have been found for the net ecosystem production (NEP, i.e., the balance between autotrophic and heterotrophic GPP) and ecosystem respiration. A positive NEP means that organic matter is either accumulated or exported (with tidal waters) when measured using an EC tower (Yan et al. 2008). These mismatches between the two estimates call for independent field experiments for the direct measurement of tide-induced lateral flows at different temporal scales (Santos et al. 2019).

Based on these considerations, this study establishes an integrated quantitative approach incorporating both modeling and field sampling for assessing the lateral detrital C exchange. To verify the effectiveness of this integrated approach, we conducted a case study in an estuarine wetland dominated by native *Phragmites australis* (hereafter *Phragmites*) and invasive *Spartina alterniflora* (hereafter *Spartina*). We hypothesized that *Spartina* invasion is coupled with lateral exchanges and thereby alters the ecosystem C cycle at various spatial and temporal scales. The application of this framework to the

case study allowed us to answer the following questions: (i) What are the relative contributions of lateral (i.e., detritus) C fluxes to the annual budget? (ii) What is the variability of lateral detrital C flux at daily, monthly, and yearly scales? (iii) How does *Spartina* invasion influence these? Sedimentation was thoroughly examined in our earlier study (Gao et al. 2020). Thus, we focused on the seasonal changes in lateral detrital C fluxes at multiple temporal scales on the difference between the EC tower technique (GPP_{EC}) and remote sensing (GPP_{MODIS}).

Methods

Study area

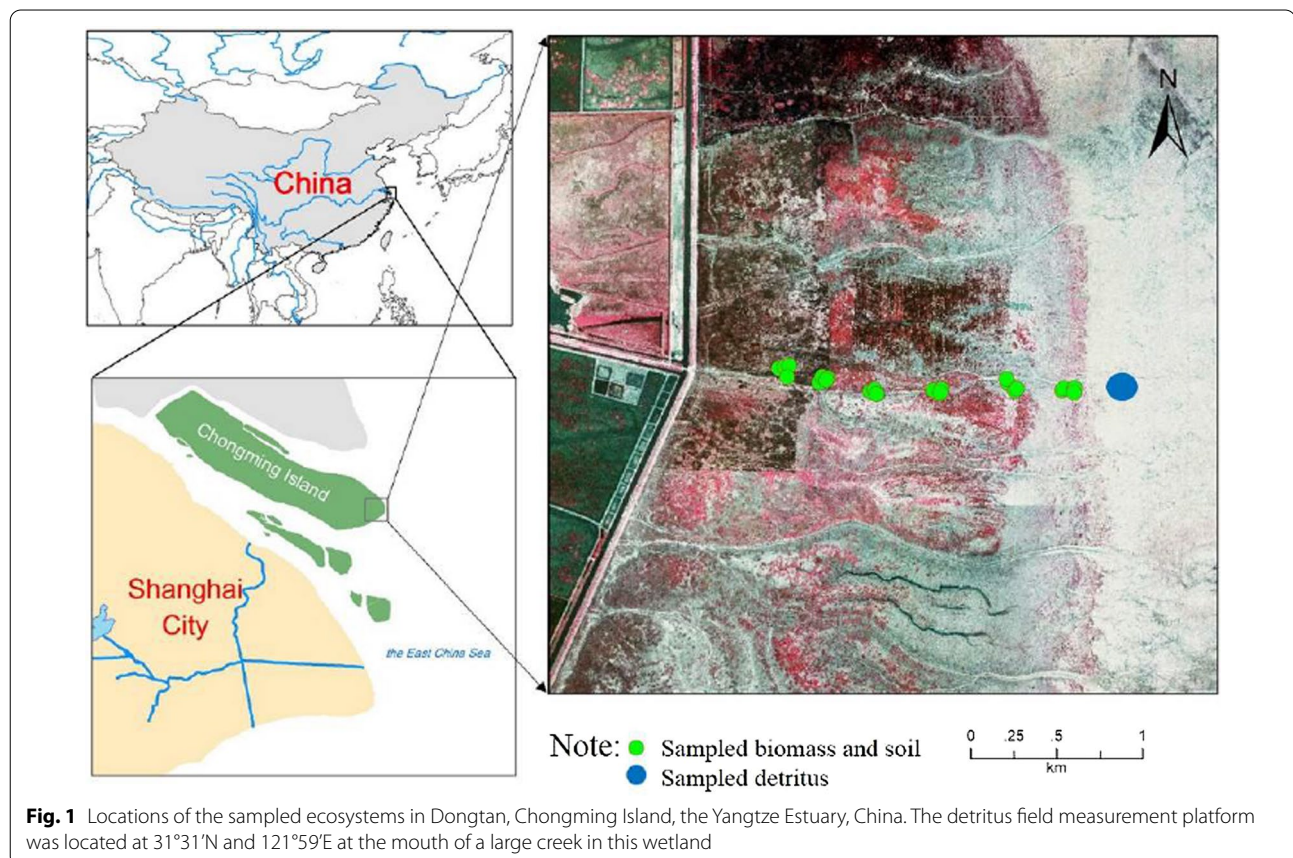
Our study area is located in the estuary of the Yangtze River ($31^{\circ}25' - 31^{\circ}38'N$, $121^{\circ}50' - 122^{\circ}05'E$), China, which is one of the broadest river mouths in the world (Fig. 1). At the time of our study, the dominant native plants were *Scirpus mariqueter* and *Phragmites*, with clear zonation of the plant communities in the vegetation area and *Spartina* has been an invasive plant in this area since 2001 (Chung 2006; Yang et al. 2017). The soil is classified as hydric, with mean (\pm SD) C storage in the top 0–20 cm of the sediment of 3.14 ± 0.05 kg C m^{-2} . The hydrology of the marsh involves a well-developed

creek system and the input of tidal water from the adjacent coast. Tides range from 4.6 m to 6.0 m above sea level during exceptional spring tides. The tides are typically semidiurnal, and most wetlands are inundated by seawater. Due to the well-developed creek system, the flow rates of the tides are typically <1.0 m s^{-1} but can reach 2.0 m s^{-1} in the main channels with a maximum of 2.45 m s^{-1} (Yang 1999). The climate of the area is characterized by substantial seasonal variation, an abundance of precipitation (1957–2192 mm), and warm temperatures (annual mean >15.0 °C) (Huang et al. 2019). The wind is typically from SSE-SE in the summer, which generates a northward longshore current, and NW-NE in the winter, which produces a southward longshore current (Guo et al. 2009). An EC tower was established near the study area to measure meteorological parameters, such as solar radiation, air temperature, humidity, wind direction, and speed (Fig. 1).

Estimating lateral C exchange

Measurement of plant biomass and primary production

A 2-km transect was established along a main tidal creek in September 2009 (Fig. 1). Six locations along the transect, spaced 300–500 m apart, were randomly selected



to measure the total C pools in the plants and soils. We selected four replicate plots at each location, and each plot was dominated by invaded *Spartina* marshes and adjacent native *Phragmites* marshes (Fig. 1). The vegetation was identified during an a priori field survey. The selection protocol for the six sampling sites was made based on surveys of the landscape along a west–east transect 100 m from the edge of the main tidal creek. At each site, the proximity of the communities was selected to minimize the spatial differences in the measurements in the estuarine wetlands. The aboveground and belowground biomass at each site was harvested in September 2009 and 2010 according to the protocol first established by Liao et al. (2007).

Four 0.5 × 0.5-m quadrats were randomly established at each sampling location and time. The aboveground biomass in the four quadrats was collected and sorted into standing biomass and dead litter. We further separated the standing and litter produced in the current year and produced in the previous year according to the litter color. All the biomass samples were immediately washed with clean water, passed through a sieve with a mesh size of 0.45 mm, and oven-dried to a constant weight at 50 °C before weighing. Due to difficulties in access and sampling, the belowground biomass was sampled only to a depth of 20 cm at the center of each quadrat at each patch after harvesting the aboveground vegetation using a large steel auger (inner diameter of 14.2 cm). The roots and rhizomes were removed before the samples were weighed. All samples were immediately washed with water and passed through a sieve (0.45-mm mesh). All the soil samples were oven-dried overnight at 80 °C to a constant weight to determine the C concentrations. The dry soil and plant biomass were ground using a Wiley mill and passed through a 100-mesh sieve. The sieved plant and soil samples were analyzed using a CN Analyzer (FlashEA 1112 Series, Thermo Inc., Italy) to determine the total C concentration.

In addition, a 0.3 × 0.3-m PVC plate was installed after the plants from an ~ 0.5 × 0.5 m area were harvested and sampled in each community in September 2009. Sediment information (e.g., sediment thickness) was collected monthly during a given phase (e.g., two neap/spring tidal cycles per month), between September 2009 and September 2010. All sediments were collected from the top of each PVC plate in September 2010. The C concentrations of the sediment samples were measured using the CN analyzer; the total C pools were calculated as 'sediments into soil' (kg C m⁻² year⁻¹). Additionally, in each plot, two pairs of 2 m long steel poles were used to measure the vertical changes in the marsh and thus verify the sediment thickness measured based on the top of PVC plates, to an accuracy of ±1 mm. The aboveground net primary

production (ANPP) was estimated by harvesting the peak standing live biomass due to the low mortality during the growing season. The belowground net primary production (BNPP) was estimated using the method proposed by Lomnicki et al. (1968).

Modeling of the estuarine C balance

The eddy-covariance method was applied to quantify the half-hourly net ecosystem exchanges (NEE) of CO₂ (F_{CO2}) and CH₄ (F_{CH4}) (Fig. 1). Daily GPP_{EC} values during the study period were calculated as the nighttime ecosystem respiration (ER) minus the daytime NEE (Reichstein et al. 2005). The processing of C flux and auxiliary micro-meteorological variables involved several steps of standard quality checks and corrections. In brief, the raw data spikes were filtered. The diagnostic signals from a sonic anemometer (CSAT3, CSI), an open-path CO₂/H₂O infrared gas analyzer (LI7500, LI-COR, Inc., Lincoln, NE, USA), and an open-path CH₄ gas analyzer (LI7700, LI-COR) were used to detect and filter out any periods of instrument malfunction with a dynamic parameter model. The turbulence data were sampled at a frequency of 10 Hz and collected by a data logger (CR5000, Campbell Scientific, Inc., USA). The measurement period for F_{CO2} and F_{CH4} was from January 2010 to December 2012. However, the quality criteria led to gaps of different durations (Detto et al. 2011). In addition, due to the quality control procedure, the rejection rates varied greatly from day to day in 2010. Therefore, to obtain reliable daily averages, F_{CH4} was calculated for the 2011 growing season in our analysis.

The GEE of C in coastal wetlands can be calculated as:

$$\text{GEE} = \text{GPP} + F_{\text{lateral}} + F_{\text{CH4}} + F_{\text{other}} \quad (1)$$

where F_{lateral} is the lateral exchange of C between wetlands and the ocean through diffusion and tidal activities, F_{CH4} is the amount of CH₄ released from anaerobic soil, and F_{other} refers to unquantified exchanges of C in other forms (Yan et al. 2008).

The half-hourly F_{CO2} and F_{CH4} were calculated and quality controlled using EddyPro software (v. 6.2.2) (LI-COR) following the workflow described by Reichstein et al. (2005) and Chu et al. (2014). The daily GPP_{EC} was then aggregated into eight-day intervals and fit to the Michaelis–Menten model.

$$\text{NEE} = R_e - \varepsilon_0 \text{PPFD} \text{GPP}_{\text{max}} / (\varepsilon_0 \text{PPFD} + \text{GPP}_{\text{max}}) \quad (2)$$

where NEE is the net ecosystem exchange of CO₂, R_e is the ER, ε_0 is the maximum light-use efficiency, PPFD is the photosynthetic photon flux density, and GPP_{max} is the maximum GPP. The uncertainties of seasonal F_{CO2}, F_{CH4}, and GEP (e.g., random, gap-filling, friction velocity

(u.) sensitivity, and GEP/ER partitioning) were similar to those described by Li et al. (2018). The energy balance closure was examined for both the annual and daily integrals of energy fluxes/storage changes (Grachev et al. 2020).

We used the MODIS remote sensing data for landscape-level GPP (GPP_{MODIS}) based on the gap-filled product MOD17A2HGF version 6. The annual composite MODIS reflectance was based on the radiation-use efficiency MODIS product (MOD15A2H). The leaf area index (LAI) and the fraction of photosynthetically active radiation (FPAR) were derived from the 8-day composite at a spatial resolution of 500 m (Running and Zhao 2019). The GPP_{MODIS} estimation depends on vegetation

characteristics (e.g., the LAI); consequently, this estimation covers neither lateral C exchange nor non- CO_2 forms (e.g., CH_4 release) (Couwenberg et al. 2011; Prince and Goward 1995).

Sampling of lateral detrital C fluxes

We measured fluxes of macrodetritus (e.g., litter) in a tidal creek during 2010. Six floating nets were placed at the mouth of a 10-m-wide creek to catch floating macrodetritus in the first 50 cm of the water column. Three nets were used to quantify detritus during ebb tides, and the other three were placed to catch detritus during flood tides (Fig. 2). The nets were composed of 2-mm

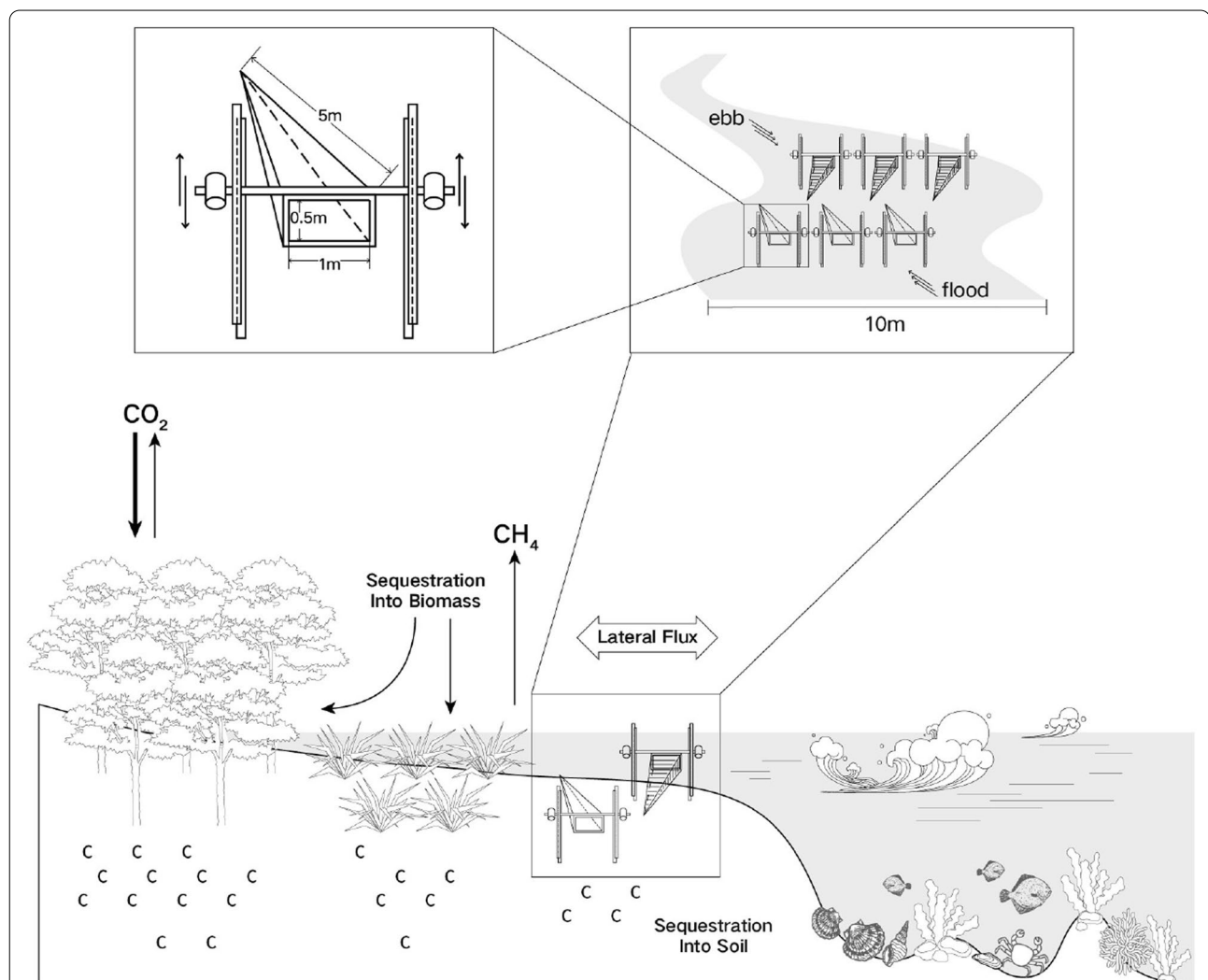


Fig. 2 Schematic diagram showing the design of nets for catching imported and exported detritus in coastal wetlands, the location of the nets, and the layout of the nets. The nets used for exported detritus were only placed during ebbing tides, and the nets used for imported detritus were only placed during flood tides to avoid disturbance. The nets were located in the same cross-sectional position of the creek, and we offset them in the diagram to make them observable

nylon mesh and were 1-m wide, 50-cm tall, and 5-m long (Bouchard 2007; Gao et al. 2018).

Considerable differences were observed when different sampling strategies were used to collect laterally transported detritus at other study sites (Table 1). For example, when integrating annual sums, the exported detritus accounted for more of the NPP over a long time scale (ca. monthly) than that over a short time scale (ca. daily) (Table 1). Therefore, field sampling strategies over multiple temporal and spatial scales for collecting laterally transported detritus are essential to minimize this uncertainty.

Trapped macrodetritus was collected, kept cool, and transported to the laboratory, where all samples were preserved at 4 °C until further processing. The collected plant materials, including both green (fresh) and yellow/dark (senescent) samples, were oven-dried at 65 °C for 48 h to a constant weight. The sieved macrodetrital C concentrations were analyzed using an automatic elemental analyzer (FlashEA 1112 Series, Thermo Scientific Inc., Italy). The amount of material trapped at each net was multiplied by ten (ratio between the net width and the creek width) to estimate the fluxes of floating macrodetritus from the studied watershed according to the analysis protocol described by Bouchard et al. (1998). The positive sign conventions indicate detrital C flux leaving the saltmarsh system, and negative sign conventions indicate fluxes into the system. Hence, a net positive value indicates a net C flux out of the marsh, and a net negative value indicates a net C flux into the marsh.

Data processing and statistical analysis

The data were analyzed for variance between tides and by season. To meet the assumptions for statistical analysis of normality and homoscedasticity, the data sets were log-transformed or cube root-transformed when necessary. Unless specified, the significance level was set to 0.05,

and Tukey tests were used to compare means. If significant differences were found, the rank order was determined using Tukey's studentized range. Differences in production between tides were tested using two-tailed *t*-tests. Differences in flood and ebb concentrations of the various forms of C were compared by using repeated measures evaluating the effects of flux direction and the month of sampling. The linear relationship between GPP_{MODIS} and GPP_{EC} , the relationship of lateral detritus flux between daily and monthly sampled fluxes, and the relationship between tidal elevation and lateral detritus flux were estimated using the R language (R Development Core Team, 2017, version 3.4.3). Linear regressions were conducted using the 'lm' function.

Results

Estimation of lateral C flux

The mean annual total plant C stock (aboveground plus belowground to a depth of 20 cm) was 0.85 kg m⁻² in *Phragmites* stands and 1.12 kg m⁻² in *Spartina* stands (Table 2). The mean annual total plant C stock allocation to belowground biomass was 54.5% in *Spartina* stands and 61.2% in *Phragmites* stands, resulting in belowground plant C stocks of 0.52 and 0.61 kg m⁻²

Table 2 Variation in the total C pools in the plants and C input by NPP calculated using data collected in September 2010 (*n* = 24, belowground biomass to a depth of 20 cm)

C pool and C input	<i>Phragmites</i>	<i>Spartina</i>
<i>Phragmites</i>		
Total plant C stock (kg m ⁻²)	0.85 ± 0.04	1.12 ± 0.06
Belowground plant C stock (kg m ⁻²)	0.52 ± 0.03	0.61 ± 0.04
Aboveground plant C stock (kg m ⁻²)	0.33 ± 0.02	0.51 ± 0.02
NPP (kg C m ⁻² year ⁻¹)	0.64 ± 0.04	0.82 ± 0.06
Sediments into soil (kg C m ⁻² year ⁻¹)	0.42 ± 0.05	0.66 ± 0.08
Sediment thickness (cm year ⁻¹)	2.1 ± 0.4	3.2 ± 0.6

Table 1 Comparison of different sampling strategies used to collect laterally exported detritus at different study sites (ANPP = aboveground net primary production)

Reference	Site	Marsh type	Sampling frequency	Contribution of ANPP (%)
Teal (1962)	Sapelo Island, Georgia, USA	<i>Spartina alterniflora</i>	Yearly	45
Palomo and Niell (2009)	Palmones River estuary, Spain	<i>Sarcocornia perennis</i> ssp.	Bimonthly	12
Wolff et al. (1979)	Oosterschelde estuary, The Netherlands	<i>Halimione portulacoides</i> , <i>Spartina townsendii</i> , <i>Puccinellia maritima</i>	Monthly	10
Bouchard et al. (1998)	Southern Normandy gulf, France	<i>Atriplex portulacoides</i>	Weekly	14
Dame et al. (1986)	North Carolina marsh, USA	<i>Spartina alterniflora</i>	Daily	< 1
Dankers et al. (1984)	Ems-Dollard estuary, The Netherlands	<i>Puccinellia maritima</i>	Daily	1
Hemminga et al. (1996)	Westerschelde estuary, The Netherlands	<i>Elymus pycnanthus</i> , <i>Scirpus maritimus</i> , <i>Phragmites australis</i> , <i>Puccinellia maritima</i>	Daily	< 0.2

in *Phragmites* and *Spartina* stands, respectively. The C concentration in fresh shoots (0.35 g C g^{-1}) was significantly higher than that in the standing litter (0.30 g C g^{-1}) ($p < 0.01$). The annual NPP (ANPP plus BNPP) was $0.82 \text{ kg C m}^{-2} \text{ year}^{-1}$ in *Spartina*-dominated communities and $0.64 \text{ kg C m}^{-2} \text{ year}^{-1}$ in *Phragmites*-dominated communities (Table 2). The total C release through lateral flows ranged from 0.21 to $0.30 \text{ kg C m}^{-2} \text{ year}^{-1}$, and the average was equal to 25.8% of NPP.

Both MODIS-predicted GPP ($\text{GPP}_{\text{MODIS}}$) and tower-observed GPP (GPP_{EC}) exhibited an apparent seasonal pattern corresponding to the growing seasonal changes in vegetation, and most GPP_{EC} values were higher than the $\text{GPP}_{\text{MODIS}}$ values with that exception of those at the beginning of the growing season (i.e., March) (Fig. 3). In addition to the difference (i.e., ΔGPP) between GPP_{EC} and $\text{GPP}_{\text{MODIS}}$, the $\text{GPP}_{\text{MODIS}}$ ($472.6 \text{ g C m}^{-2} \text{ year}^{-1}$) was 73.0% of GPP_{EC} ($646.9 \pm 70.7 \text{ g C m}^{-2} \text{ year}^{-1}$) during the 2010 growing season (Fig. 3a). These figures were essentially consistent with the aboveground plant C stock measured by harvesting the biomass at peak vegetation growth (Table 2). In contrast, we detected more $\text{GPP}_{\text{MODIS}}$ during the pre-growing season period, consistent with the magnitude of the lateral detrital C flux observed in the tidal creek in March (Fig. 4). Additionally, the annual CH_4 emissions measured by conventional eddy covariance techniques (March 23, 2011–December 31, 2011) were $17.9 \pm 3.7 \text{ g C m}^{-2} \text{ year}^{-1}$ and exhibited a distinct seasonal pattern. These results suggest that the emission of C in non- CO_2 form (i.e., CH_4) accounts for 2.8% of the GPP_{EC} (Fig. 3) and allow us to calculate the actual lateral C flux caused by tides in the following section.

Observation of the lateral detrital C flux

A significant correlation was found between imported and exported detritus flux on the daily and monthly scales. In addition to the flux that resulted from tidal activities, the C imported by tides could also contribute to the exported C. The daily detritus flux appeared to exhibit a left-skewed distribution over the year, albeit with several exceptions (Additional file 1: Fig. S1). On average, the amount of detritus exported to the ocean was higher than that imported to the land. The net positive flux (i.e., more detritus leaving the wetlands) appeared to be related to daily tides. Although nearly 90% of the daily detritus flux values were between -0.16 and $0.16 \text{ kg C m}^{-2} \text{ day}^{-1}$, they could also exceed $0.16 \text{ kg C m}^{-2} \text{ day}^{-1}$ (Fig. S1).

The lateral flux based on monthly sampling (i.e., once a month) was higher than that based on daily sampling (i.e., the sum of daily sampling), particularly in March and October (Fig. 4a). In addition, the daily sampling

strategy resulted in a lower annual sum than the monthly sampling strategy for both input and output. Furthermore, the monthly net value (output – input) based on the daily sampling strategy was lower than that based on the monthly sampling strategy (Fig. 4a), except in July. The annual net flux obtained with the daily and monthly sampling strategies was $1.13 \text{ kg C m}^{-2} \text{ year}^{-1}$ and $1.96 \text{ kg C m}^{-2} \text{ year}^{-1}$, respectively. This discrepancy implies that 42.3% of the annual total can be due to daily differences, even though a high correlation ($r^2 = 0.73$, $p < 0.01$) was found between the estimates (Fig. 4b).

The relationship between lateral detritus fluxes and tidal activity seemed statistically non-significant between the two sampling methods (Fig. 5). However, when the exceptional month of March was not considered, there was a significant correlation ($r^2 = 0.62$, $p < 0.05$) between the monthly lateral detritus fluxes based on daily samplings and the maximum tidal height (Fig. 5a). On the other hand, a similar relationship was not detected in monthly sampled data (Fig. 5b).

Discussion

C budget of estuarine wetlands

The outwelling hypothesis states that salt marshes produce more organic matter than can be utilized within the system and that this excess material is exported to coastal waters (Das et al. 2011). The lateral C fluxes described in this manuscript have rarely been studied in concert with and in the context of the vertical flux of C (i.e., both F_{CO_2} and F_{CH_4}). To better understand the relative importance of land–water C fluxes, we must move toward research that fully integrates the C budget across terrestrial ecosystems and coastal waters. The estimates of C fluxes were not only based on biomass and primary production but also based on tower-based measurements (F_{CO_2} , F_{CH_4}) and MODIS time series direct measurements of the lateral detrital C flux. Most importantly, the hydrological processes dominated by tidal activity can significantly affect the magnitude, direction, and dynamics of lateral fluxes. Our previous findings indicate the occurrence of a bidirectional C process, such as detritus at a daily scale, is non-significant (Gao et al. 2018). Our study also suggests that the net detrital C export exhibited a bimodal seasonal pattern over a year in a typical coastal salt marsh of the Yangtze River estuary. Unfortunately, previous studies on the lateral flows of C were conducted periodically for CO_2 only. Without the inclusion of methane (CH_4) (Li et al. 2018), we were prevented from reaching a mass balance of marsh C. This case study illustrates that an integrated framework incorporating modeling and field sampling can quantitatively assess lateral detrital C transport processes across the terrestrial-aquatic interface in estuarine wetlands.

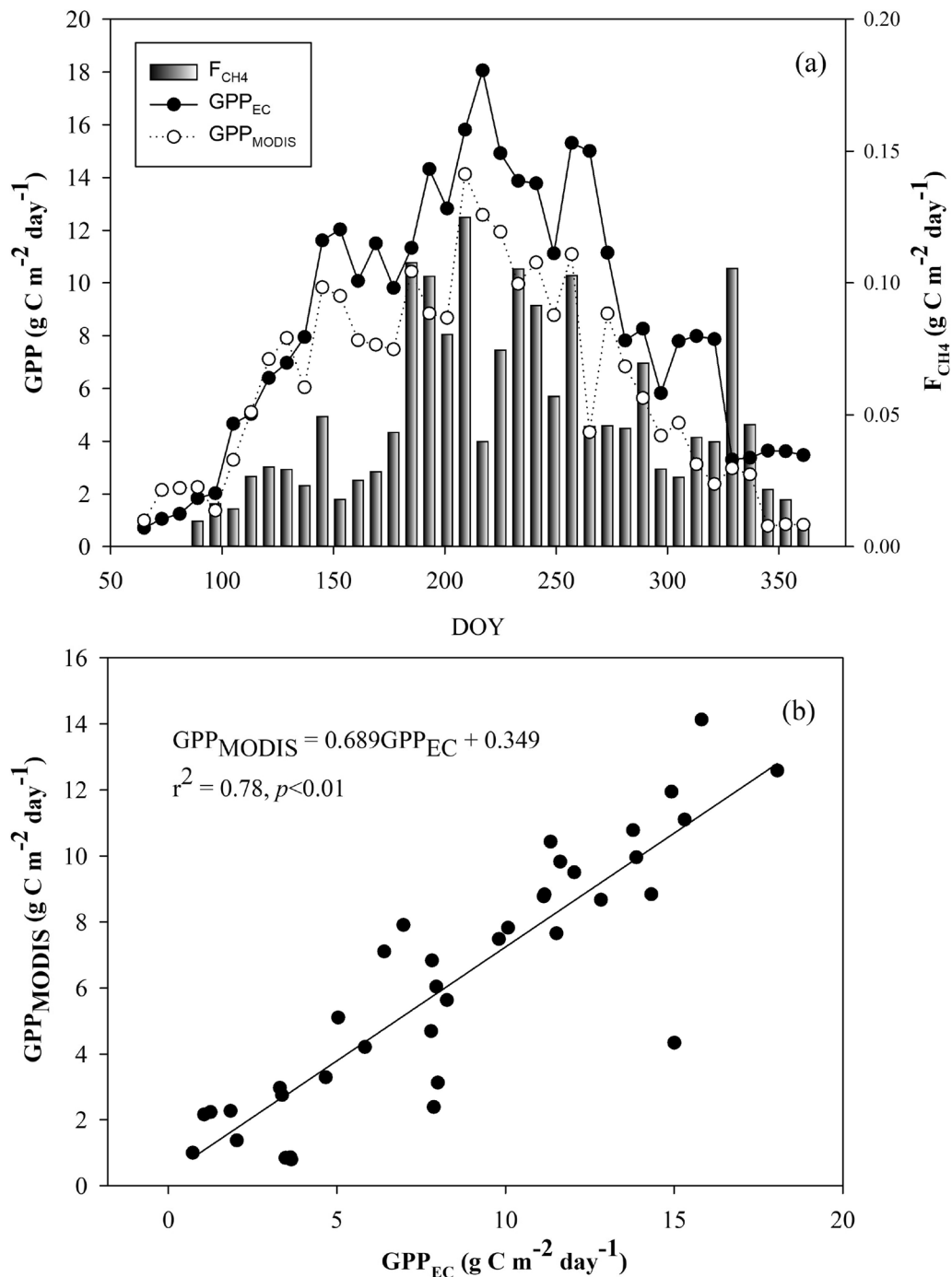


Fig. 3 Seasonal changes in gross primary production from eddy covariance towers (GPP_{EC}), MODIS-based GPP ($\text{GPP}_{\text{MODIS}}$), and net ecosystem exchange of CH_4 (F_{CH_4}) (DOY equals day of year) (a) and the linear relationship between GPP_{EC} and $\text{GPP}_{\text{MODIS}}$ (b). GPP_{EC} and $\text{GPP}_{\text{MODIS}}$ were estimated during the 2010 growing season

Our current and previous studies in the same tidal wetland (Gao et al. 2018; Guo et al. 2009; Li et al. 2018; Yan et al. 2008) provide rich knowledge and data for the total C budget of this coastal wetland in the context of the

outwelling hypothesis. On an annual basis, the vertical C budget (F_{CO_2} and F_{CH_4}) revealed that the marsh represents a significant C sink of $629.0 \text{ g C m}^{-2} \text{ year}^{-1}$ (Fig. 6), which is inconsistent with the lateral C accumulation

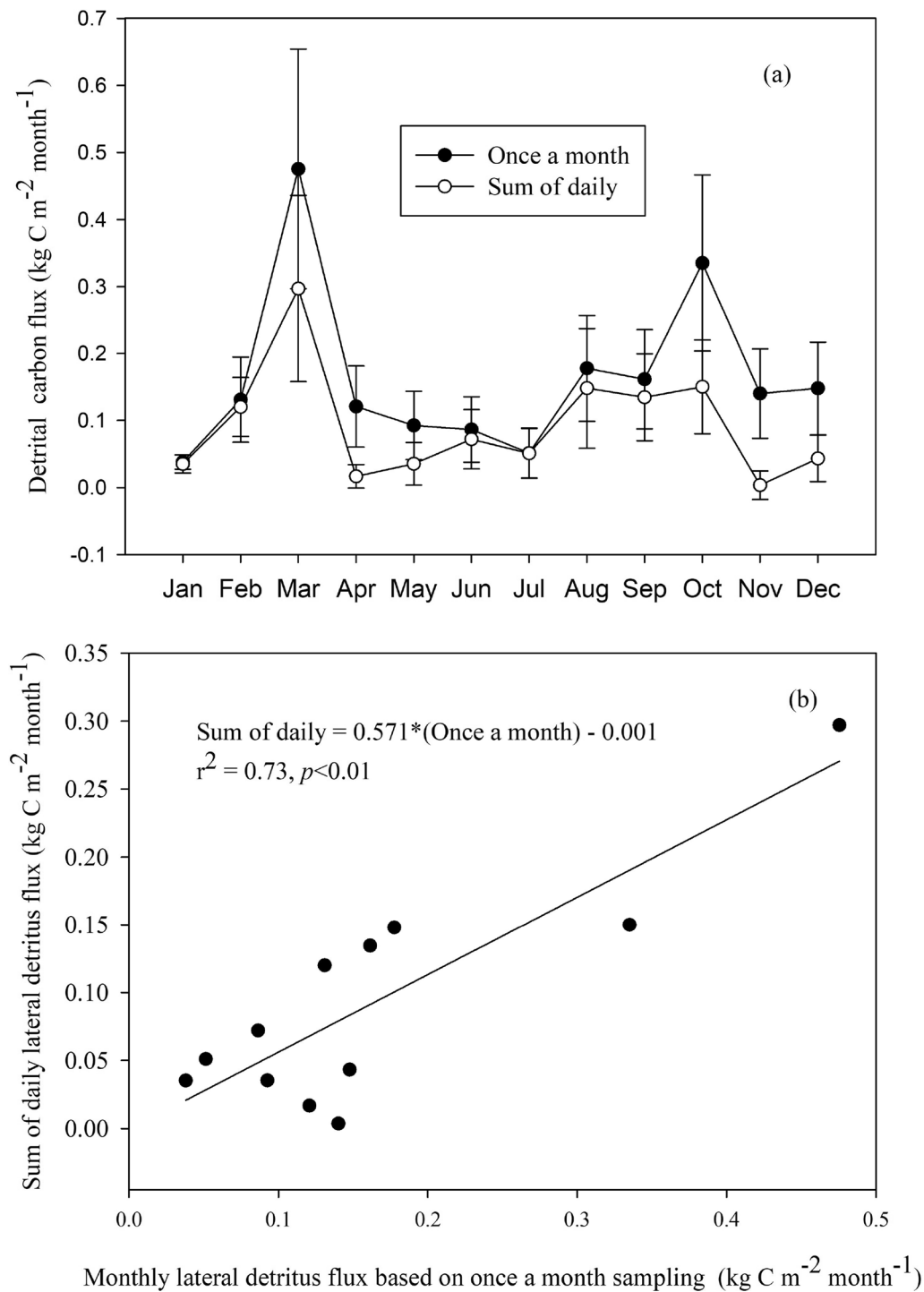


Fig. 4 Comparisons (a) and the linear relationship (b) of lateral detritus flux between daily and monthly totals

trend. An analysis of the lateral C flux revealed that the net hydrologic C fluxes varied considerably within the ecosystem between the two communities. Moreover, F_{CO_2} largely compensated for F_{CH_4} , the lateral detrital C

flux, and the input sediments into the soil and led to near neutral net hydrologic C fluxes in the *Phragmites*-dominated area (Fig. 6a). However, the lateral C balance transitioned from indicating that the *Phragmites*-dominated

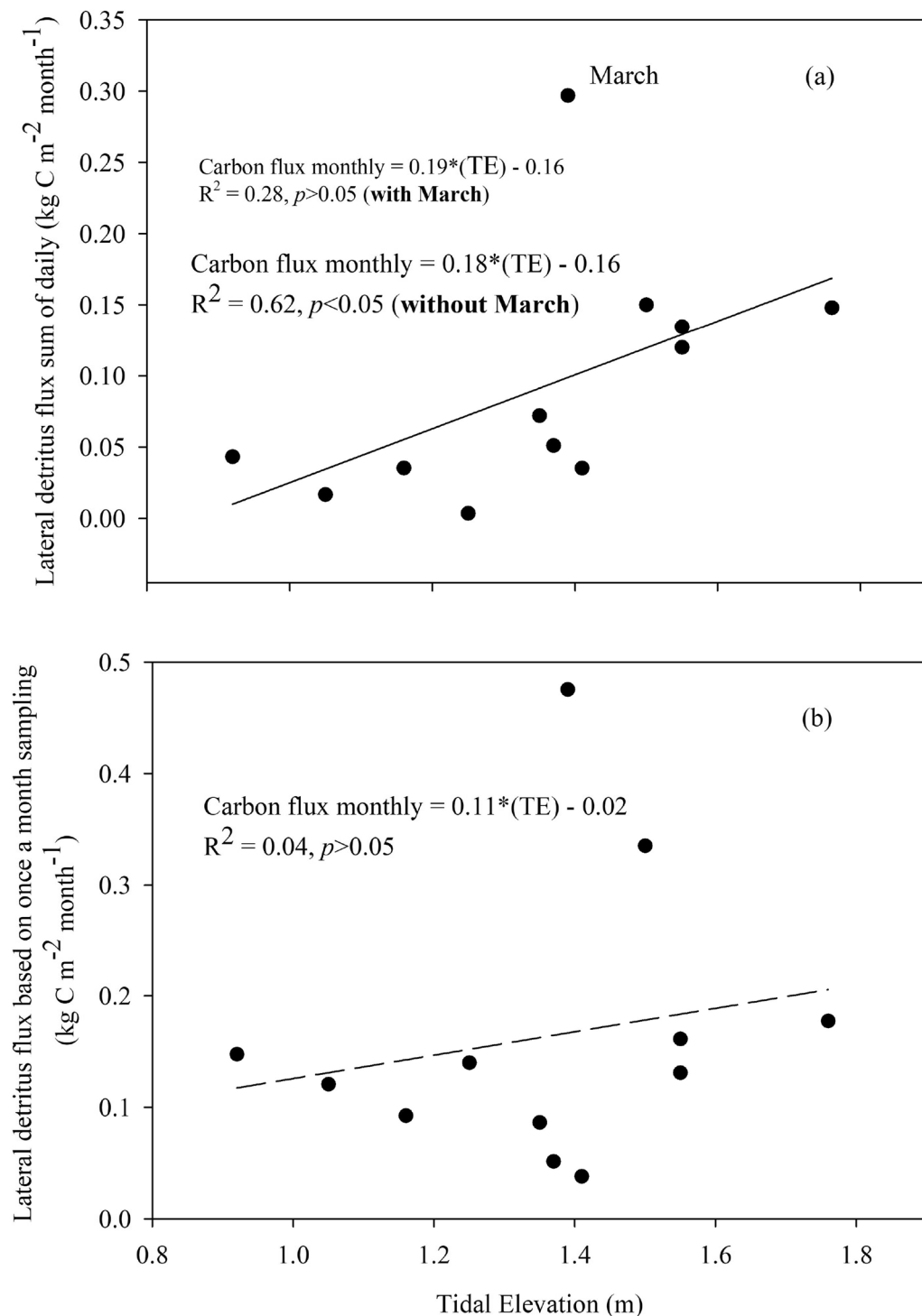
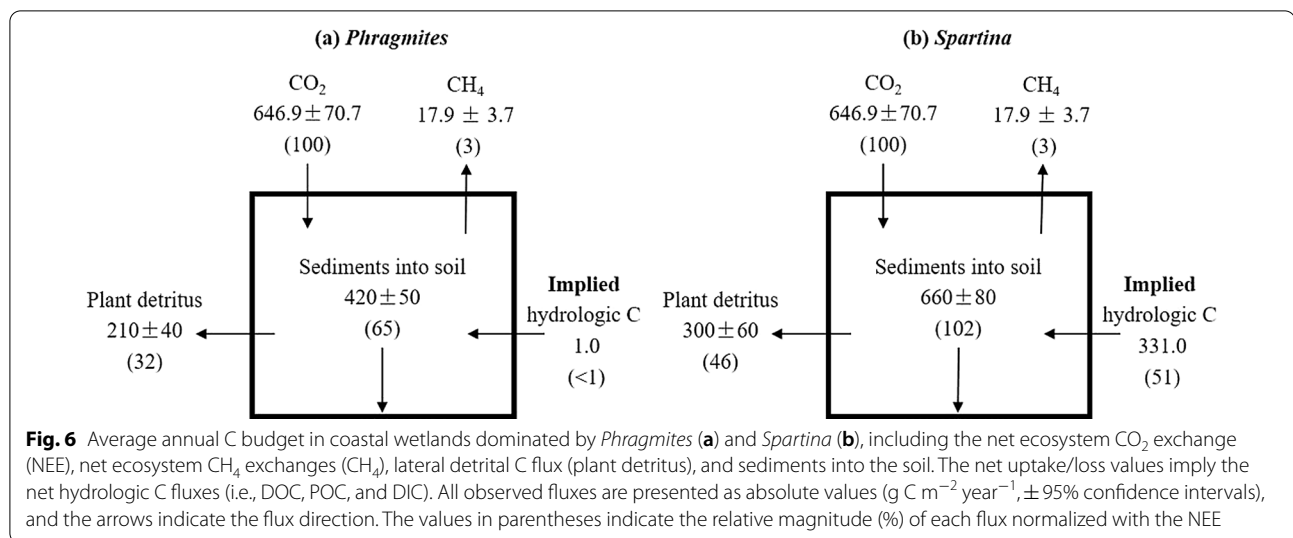


Fig. 5 Linear relationships between tidal elevation and lateral detritus fluxes based on the daily sum **(a)** and monthly total **(b)**

communities were a C source ($209.0 \text{ g C m}^{-2} \text{ year}^{-1}$), which suggested that *Spartina*-dominated communities are a C sink ($-31.0 \text{ g C m}^{-2} \text{ year}^{-1}$), and 51% of NEE originated from lateral movement (Fig. 6b). Our previous

studies indicated that invasive *Spartina* obtained extra subsidies during hydrologic processes in transporting C among ecosystems (Gao et al. 2020). Presumably, the shorter, denser stems of *Spartina* might have a much



better chance of accelerating sedimentation than the meter-high stems of the native *Phragmites*. It is also possible that the shorter, denser vegetative cover of *Spartina* tends to slow tidal flow down to a greater extent and captures finer sediment grain size during relatively faster and more turbulent flow conditions (Gao et al. 2016). These two components may be responsible for differences in sediment dynamics between invasive *Spartina* and natural *Phragmites* at high flow rates. Nevertheless, the results of closing C budget calculations obtained through this coupled framework are still subject to some uncertainties arising from several sources. Therefore, this scenario needs to be adequately analyzed by continuously measuring the surface sediment composition of the litter mass of the two species.

Overall, our findings highlight the importance of closing the C budget of estuarine wetlands in the context of a terrestrial-aquatic continuum. The C loss via CH₄ emissions may not be compensated by the net uptake of CO₂, showing the significance of hydrologic flows in leaching C from coastal wetlands. Most importantly, robust regional and global modeling/upscaling requires an accurate estimation of terrestrial GPP in various communities (Yuan et al. 2014). The GPP estimates of different communities have varied widely depending on the model used. However, the selection of different C models (e.g., linear or quadratic) may exert a significant effect on estimation and interpretation (e.g., Law et al. 2000 and Xiao et al. 2004) (Table 3). Our earlier study found that the predicted GPP from the light-use efficiency model (GPP_{MODIS}) underestimated GPP relative to that observed from eddy flux tower measurements (GPP_{EC}). This study improved the accuracy of the GPP estimates by 8.0–19.6% (i.e., from 53.4–65.0% to 73.0%) with an

Table 3 Comparison of light-use efficiency models for gross primary production (GPP)

Model	FAPAR	ϵ_g	ϵ_0	Reference
TURC	$f(NDVI)$	ϵ_0	0.24	Ruimy et al. (1994)
GLO-PEM	$f(NDVI)$	$\epsilon_0 \times T \times SM \times VPD$	0.14	Prince and Goward (1995)
MODIS-PSN	$f(LAI)$	$\epsilon_0 \times T \times VPD$	0.22	Running et al. (2004), Running and Zhao (2019)
3-PG	$f(LAI)$	$\epsilon_0 \times T \times SM \times VPD$	0.48	Law et al. (2000)
VPM	$f(EVI)$	$\epsilon_0 \times T \times SM \times W \times P$	0.48	Xiao et al. (2004)

GPP = $\epsilon_g \times FAPAR \times PAR$ or GPP = $\epsilon_g \times FAPAR_{PAR} \times PAR$. The scalars for light-use efficiency (ϵ_g) include temperature (T), soil moisture (SM), water vapor pressure deficit (VPD), canopy water content (W), and leaf phenology (P). FAPAR fraction of absorbed photosynthetically active radiation, NDVI normalized difference vegetation index, LAI/leaf area index, EVI enhanced vegetation index, ϵ_0 maximum light-use efficiency

updated version of the MODIS data (Fig. 3). In turn, the difference between GPP_{EC} and GPP_{MODIS} (ΔGPP) was generally compatible with our estimates based on biomass and primary production (Fig. 6). In this study, the effect of the annual CH₄ release was successfully quantified as a variable predicting the difference between the two GPP estimates, according to Eq. (1), which allowed us to calculate the actual lateral C movement. This finding means that C lost as CH₄ altogether led to ~2.8% of the C uptake via F_{CO2} on a C balance (Fig. 3b). The CH₄ emissions observed in this study may only slightly offset the discrepancy in our marsh C budget, aside from uncertainties originating from both GPP_{EC} and GPP_{MODIS} (Mittra et al. 2020). However, we note some limitations in our research approach regarding the application of the light-use efficiency model method to tidal wetlands. These simplifications and the weakness of the light-use

efficiency model in tidal wetlands could introduce some uncertainties in the GPP simulation results and eventually influence the C transfer flux calculations (Table 3).

However, the issues related to the uncertainties (e.g., analytical, instrumental, and methodological) and challenges made a direct comparison of these reports to our annual estimated hydrologic C questionable. First, all of the measured C fluxes in the lateral C budget (e.g., detritus, POC, DOC, and DIC) have very different sources and magnitudes of uncertainty. This input uncertainty resulted in significant uncertainty in closing the marsh C budget when solving lateral C flows. Furthermore, wetland C cycling and annual C budgets may vary drastically among different communities. It should be noted that *Spartina* invasion also affected F_{CO_2} and GPP and led to an enhanced CO_2 uptake rate. Second, among all of the sampling locations matching the footprint and the catchment, the sampling frequency adopted in integrating the vertical and lateral components should have a minor influence on the interpretation of our marsh C budget. Third, there are knowledge gaps in the adequate quantification of C loss during the nongrowing season. Even though we have carefully examined and estimated the different sources of the uncertainties, unknown uncertainties remain that cannot be assessed based on our current design (e.g., energy balance closure) (Cui and Chui 2019). Furthermore, this includes some C fluxes and/or storage changes that were unaccounted for and not quantified in our budgets, such as the belowground biomass below a depth of 20 cm and C within the water column.

Despite this data gap, the general framework and methodology presented here are applicable and suitable for other, sizeable watersheds with more complicated land-sea interactions. According to Eq. (1), the mismatch between GPP_{MODIS} and GPP_{EC} potentially indicates that the lateral C flux (i.e., detritus in hydrologic flow paths) caused by tides accounted for 24.2% of the GPP_{EC} ($646.9 \text{ g C m}^{-2} \text{ year}^{-1}$), which was compatible with the 25.8% obtained based on biomass and primary production. However, C assimilated through photosynthesis that eventually entered the soil could have increased the sediments at a regional scale. The CH_4 flux is also an essential component of the wetland C budget (Parker et al. 2018). The sediment records obtained by our team from the same tidal wetland also suggest that the marsh accumulated a considerable amount of C (Gao et al. 2020), which implies that an unknown portion of the deposited C originated from allochthonous C sources. Thus, we revealed the importance of including lateral detrital C fluxes in wetland C budgets, particularly for those characterized by bidirectional C processes (i.e., simultaneous lateral C exchanges and sediment deposition). Furthermore, the coastal wetland C cycling and annual C budgets may

vary between years. Therefore, multiple-year datasets are necessary to further determine the extent to which these C fluxes (i.e., F_{CH_4} , lateral C exchanges, and sediment deposition) and their budgets contribute to the difference between GPP_{EC} and GPP_{MODIS} at the annual scale. Moreover, the light-use efficiency model itself contains empirical formulas and complicated parameters to enable simplification. Thus, we suggest that future applications incorporate simplifying assumptions and omitted calculations into the presented framework for other larger-scale basins.

Temporal and spatial lateral C fluxes across landscapes

A significant challenge related to the outwelling hypothesis has been understanding how detritus-derived organic matter can represent the lateral fluxes determined by tidal activity. The present study suggests that the direct measurements involved in the daily sampling strategy are rarely successful, particularly during storm tides when the salt marsh is entirely covered by water. In practice, it is impossible to perform direct measurements during storm tides because these events occur at time scales much longer than the daily tidal time scale, on which the daily sampling strategy is biased (Winter et al. 1996). In addition, accessibility and the significant time and staffing commitments needed for collecting samples and laboratory testing were significant constraints in this study, and these factors will likely persist in future applications.

Consequently, relatively few direct measurements have been conducted during storm tides in coastal/estuarine wetlands because acquiring ground data in these ecosystems is highly costly in terms of both time and labor due to access difficulties (Wolff et al. 1979). Overall, the mismatch in temporal resolution also poses difficulties in comparing the annual lateral detrital C budget. Nonetheless, our limited efforts (especially considering that our daily measurements were not extremely continuous) reveal that detritus-derived organic matter may not be exported in high amounts, as expected (Hunsinger et al. 2010).

Our previous study found that monthly lateral green (fresh) detrital C was highly correlated with the height of tides in the daily sampling strategy, but a similar relationship was not observed for yellow/dark (senescent) detritus (Gao et al. 2018). In this study, however, distinguishing green detritus from yellow/dark detritus seemed hard to achieve, particularly with the monthly sampling strategy, because the green detritus turns yellow/dark after a long time (ca. a month). When pooling both types of detritus together, the lateral detrital C flux was not significantly correlated with tidal elevation (Fig. 5), except for the exceptional month of March, which was not considered in the daily sampling strategy (Fig. 5a). This

finding is actually comparable with our previous results (Gao et al. 2018), which suggested that it is necessary to sort different types of detritus when linking lateral detrital C flux to the seasonal patterns of tidal events. Exportable green detritus remains relatively stable in any given period, whereas the amount of exportable yellow/dark detritus fluctuates due to the process of accumulation and decomposition. Moreover, increased sampling over a longer time (ca. an entire season) would benefit future studies using this proposed framework. Automatic sampling instruments also could be adopted in future studies to ensure higher sampling rates with shorter space distances between each site to better capture the spatial-temporal variability.

In contrast, it is possible that the departure or re-entry of that trapped macrodetritus was prevented because the macrodetritus collected on a short time scale was removed from the nets immediately after the tides (Dame et al. 1986). However, it is also possible that trapped macrodetritus may depart from the floating nets and be recaptured by the nets with a change in the tide level (Dankers et al. 1984; Lehman et al. 2015). The ecosystem does not stop at the tidal limit. It comprises the whole primary creek catchment, including the creek and its tidal wetlands, the estuarine wetlands, and the seagrass in the coastal waters. Very little is known about the quantity and proportion of recaptured macrodetritus, but this component could be critical to estimating the lateral matter budget (Evans and Thomas 2016). Instead, the proportion of recaptured macrodetritus has to be determined indirectly using appropriate methods. Thus, the collection of time-series measurements in this study that can capture short-duration events such as storms may support the argument that a simpler monthly time scale can better reflect the actual situation of net litter flux. Moreover, the tidewater could not inundate the saltmarsh but only carried off the macrodetritus in the tidal creeks. This information could indicate that a marsh functions as an importer or exporter of detritus in association with different temporal sampling scales. These measurements will also contribute to a greater understanding of the variation in lateral detrital C fluxes between average and storm conditions, which was assumed to be linear in this study.

The storm conditions were neglected due to the difficulty of obtaining data under extreme weather conditions, such as severe storms. However, most daily transport may occur during these extreme events (Zhao et al. 2009). Thus, our results demonstrate that evaluations of the lateral transport of detritus involving the sum of daily measurements might be less reliable than conclusions about transport based on a monthly scale. Furthermore, other studies propose that for marshes at a higher

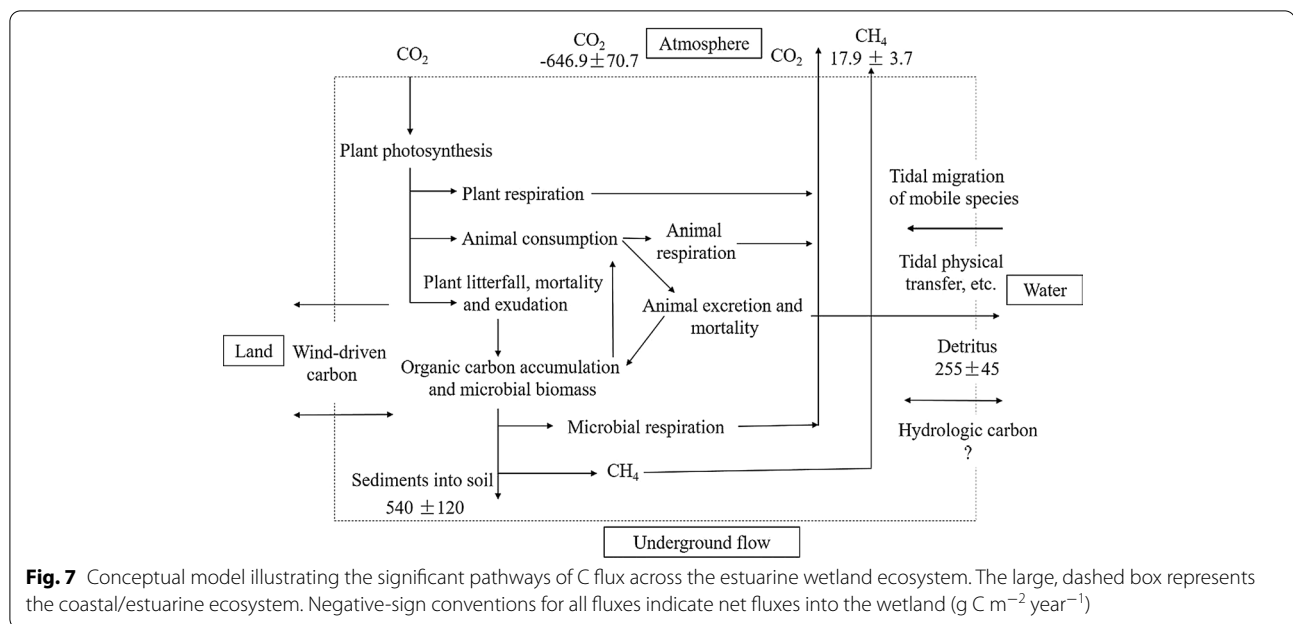
elevation, the export of macrodetritus is dominated by occasional storm tides. As a result, the net export could be six times higher than the largest import (Wolanski 2016).

Consequently, we propose that understanding and modeling the stability of detritus moved by storm tides is a process of great interest in the study of lateral matter flux (Rahaman et al. 2013). The role of lateral C flux over time is another ecological aspect lacking clear and consistent evidence. However, performing independent calibration for storm processes to improve the hydrological simulation process may dramatically decrease the uncertainty of the model simulations.

Implications for hydrologic C fluxes

We propose that the exploration of methodological advances and adequate research frameworks that can be used to evaluate cross-ecosystem C flows is urgently needed, particularly in terms of the continuous measurement of hydrologic C fluxes (Fig. 7). Most studies exploring land-to-water C flux have focused on hydrologic C flux measurements (i.e., DOC, POC, and DIC) (Fagherazzi et al. 2013). Understanding the mechanism through which the C pool moves from land to water is central to determining the fate of this C and its impact on the function of recipient aquatic ecosystems (Abdul-Aziz et al. 2018). For example, C that is laterally transported as POC and/or DOC, rather than as detritus, may only be available for microbial uptake and geological mineralization. When the different sources of hydrologic C fluxes were estimated, there remained uncounted (or unknown) uncertainties that could not be assessed based on our current design, such as the temporal dynamics in tidal C contents (Fig. 7). For example, the eddy flux tower data used for the light-use efficiency model calibration and validation for the whole watershed may also introduce uncertainty. When extended to other coastal/estuarine wetlands, this uncertainty could be reduced by using more observation station data at the calibration step.

Similarly, plant-related detritus can also be transformed into microbial food webs along a possible continuum via interaction with mineral incorporation and plant-soil-microbe feedbacks and become available for eventual sequestration in the adjacent ocean (Swain et al. 2015). Indeed, our study showed that the hydrologic processes transported $2.89 \times 10^9 - 4.13 \times 10^9$ g C year⁻¹ in the form of detritus from the coastal wetland into the East China Sea, and 13.78 km² was quantified in this intertidal zone (Zhao et al. 2008). On average, the C inflow was equivalent to a net lateral flux of up to 4.56×10^9 g C m⁻² year⁻¹ to the catchment in the watershed from the nearby aquatic ecosystem in the form of hydrologic C fluxes.



However, compared with numerous studies directly measuring the hydrologic C flux in the estuarine area of the Yangtze River (e.g., Wu et al. 2015; Wang et al. 2012), hydrologic C fluxes obtained using our mass balance estimation are approximately three orders of magnitude lower. While we have carefully examined different sources of uncertainties (e.g., methodological) in hydrologic C fluxes, there are two components that account for the significant quantitative difference. First, our interpretation of lateral transport (i.e., allochthonous C) reveals the significance of a bidirectional C process (e.g., the inputs/outputs of different lateral hydrologic C forms) in the terrestrial-aquatic continuum. Most of the work with hydrological C fluxes has focused on the flow rates and concentrations of total suspended matter. More importantly, these kinds of estimation efforts emphasize a transfer of materials out of the basin; i.e., aquatic ecosystems (e.g., rivers, wetlands, and lakes) merely convey terrestrial C to the ocean. However, in a salt marsh at the land–water interface, hydrologic C transported out of the marsh may remain in seawater not far from the marsh and might be transferred into the marsh during flooding and out during ebbing several times. Thus, the net result was clearly lower than one-way flow estimation. Second, there remain uncertainties that cannot be compared based on our current framework, such as the difference in the watershed between the two estimation methods. For example, the major hydrologic C sources for directly measured studies are the entire watershed of the Yangtze River. In contrast, this mass balance method is applied to evaluate the contribution of hydrologic C

laterally transported from the source in this 13.78- km^2 intertidal zone. It appears that this evaluation is inconsistent with previous observed values, but we believe that the next step is to establish explicit cross-ecosystem C budgets, including the calculation of essential quantities (e.g., bidirectional lateral DOC and POC transport) (Ganju et al. 2019). However, although this may lead to difficulties when applying this method to more complicated and larger catchments, the insights gained in this analysis demonstrate the advantages of quantifying the impact of tidal activities on lateral detrital C transfer.

This study also set the stage for a new research agenda to extend the outwelling hypothesis (Loreau et al. 2003). Despite the large variability among landscapes and over time, global estimates of the emissions and storage of C species associated with coastal and estuarine discharge to the ocean can be used to effectively constrain the magnitude of the global flux of C from terrestrial to aquatic ecosystems (Fig. 7). Many empirical examples supporting the outwelling hypothesis are systems with landscape boundaries between them (Dinsmore et al. 2010). The quantification of catchment features is also useful, particularly when considering regional cross-ecosystem material pools and the regional energy balance (Soininen et al. 2015). For example, when integrating vertical and lateral components, it should be noted that discrepancies among different communities in terms of the sediment reveal the uncertainties and challenges involved in estimating hydrologic C flows (Fig. 7). If 10% of the sediment originates from hydrologic C inflows (DOC + POC), the hydrologic C fluxes would increase by approximately

42–66 g C m⁻² year⁻¹. Even a small change in the C burial rate could translate to considerable changes in the magnitude and direction of hydrologic C flux. New methods combining isotopic data on temporal trophic cascades to estimate cross-ecosystem C flows would similarly round out our knowledge of spatial flows (Sippo et al. 2019). However, the source areas of sediment identified based on radioactivity dating at such short-term and local scales are challenging to define and estimate. Therefore, a much longer observational period and multiple approaches are needed to establish an overall C balance; in summary, challenges remain in the integration of these vertical and lateral components into a spatially and temporally comparable framework (Fig. 7). In addition, the integrated framework can be supplemented to make precise forecasts for the process of lateral detrital C transfer with the ultimate aim of proposing optimization management measures for sustainable carbon-neutral development.

As our understanding of lateral C flux through hydrologic processes in marine surface waters improves (e.g., Tranvik et al. (2009) and Drake et al. (2018)), estimates of C flux across the terrestrial-aquatic interface continue to be revised, potentially upward. Based on a recent assessment performed by Drake et al. (2018), an annual C export of 5.1 Pg year⁻¹ along a land-to-water path was identified, which is much more than twice the 1.9-Pg estimate presented a decade before by Cole et al. (2007). This broad-scale, global estimate can still obscure the fact that the mechanism through which terrestrial C is transported to aquatic ecosystems varies enormously across landscapes and time due to knowledge gaps and substantial uncertainties in the quantification of lateral C export. However, due to the regional variation in aquatic ecosystem function, hydrologic lateral C exchanges may serve as essential regulators in regional and global C cycling (Coch et al. 2018). To date, C cycling and perturbations caused by climate change, broad-scale changes in biogeochemical cycles, and extreme tidal storms remain understudied. Macrodetritus can be reliably trapped only when the tidal height is more than 1.0 m and can rarely be trapped when the elevation is less than 0.8 m (Gao et al. 2018). Overall, the possibility of incorporating all salient factors (e.g., storms) in the case study in addition to land-sea interactions should be explored in future analyses.

With regard to the seasonal pattern, the exceptional month of March marked not only the end of the export of yellow/dark detritus (senescent detritus) but also the beginning of the export of green detritus (fresh detritus). Plant litter is mainly produced in the winter when the aboveground parts of the plants die, and this material commonly accumulates in wetlands. This mortality pattern implies that, regardless of the cause, the pattern

accounts for the massive amount of plant litter biomass that can be exported due to a single storm (Osburn et al. 2019). For example, when March was not considered, the monthly sum of detritus calculated according to the daily sampling strategy was positively correlated with the tide height (Fig. 5a). After over-marsh tides, a large part of the detritus was transported by ebb tide within a short period after high tide. Therefore, the conclusion that significant annual exports occurred during several storm tides appears warranted. The variability in cross-ecosystem C flows could be more strongly related to the catchment characteristics of the region and the amount of tidal water that acts as a driver than local within-creek elevations (Sousa et al. 2017). Therefore, we emphasize that the quantification of contingencies and the size of tidal waters at larger spatial and temporal scales may be more appropriate and more feasible for identifying cross-ecosystem frameworks than measuring snapshot C fluxes based on water samples (Gounand et al. 2017). These steps will make significant additional contributions to the comprehensive understanding of the outwelling hypothesis in different C forms (e.g., DIC, DOC, POC) under the influence of natural factors.

The cross-ecosystem perspective provides a robust theoretical framework for addressing the outwelling hypothesis (Gravel et al. 2010). We further suggest that the cross-ecosystem framework could be the basis for a new field of integrated spatial ecosystem ecology that promises novel fundamental insights into the dynamics of ecosystems from the local to the global scale for predicting the consequences of altering the fundamental processes of cross-ecosystem C flows (Maxwell and Silva 2020). However, the estimate of yearly lateral transport according to the sampled tides was not very accurate in terms of annual flux. Because the lateral transport during several storm tides could not be quantified due to the sampling schedule, tidal water sometimes remained in the marsh for more than one daily tide. Additionally, during one storm tide, 50–100 times as much tidal water remained in the marsh as during a normal tide (Dhillon and Inamdar 2014; Ridd et al. 1988). Therefore, inaccuracies in the estimates of storm tides could result in significant variations in the yearly budget estimates. Hence, we note some limitations in our research approach associated with the appropriate time frame for detecting exceptional cases (Chen et al. 2018).

Further research, particularly on the transport and speciation involved in land-to-water C flux and the total C budget, is fundamentally important to establish a comprehensive regional C budget and enhance our understanding of these processes (Figs. 6 and 7) (Mfilinge et al. 2005). Furthermore, remote sensing and long-term records of C stocks and fluxes should be employed to

examine how these co-occurring factors have simultaneously affected terrestrial-aquatic C flux over decadal time and regional scales. Overall, measurements of vertical CO₂ and CH₄ fluxes made in concert with estimates of lateral DOC and POC production and detrital C flux will significantly enhance our understanding of this issue. A better understanding is essential given that changes in discharge across the terrestrial-aquatic interface appear to exert dramatically different impacts on hydrologic lateral C export (Alongi 2014). However, the projected POC remained inconsistent along the aquatic continuum and provided a valuable opportunity to examine the response of marsh C cycling and the C budget. Thus, the net contribution of these hydrologic C fluxes was then calculated according to the residuals of the two large and opposite fluxes (flooding and ebbing). Our report suggests that monitoring efforts that appropriately capture the lateral flux dynamics of all C species over multiple temporal and spatial scales and incorporate hydrologic regime shifts are a clear priority for future research. In parallel, the theoretical framework must account for the respective spatiotemporal scales of the quantitative information regarding the frequency at which these naturally cross-ecosystem C flows occur in both donor and recipient ecosystems to appropriately describe the flows linking ecosystems of different sizes (Sitters et al. 2015).

Conclusions

By coupled modeling and field sampling, this study estimated the lateral detrital C exchange based on GPP with tower-based measurements and MODIS time series and CH₄ outgassing and based on biomass and simultaneously measured the lateral detrital C flux to characterize the relative contributions of lateral (i.e., detritus) C fluxes to the annual marsh C budget. In conjunction with those obtained in other studies, our findings suggest that the lateral C flux (i.e., detritus in hydrologic flow paths) caused by tides accounted for 24.2% of the GPP_{EC}, which is compatible with the value of 25.8% based on biomass and primary production. However, the direct measurement of lateral detrital C flux in the tidal creek indicated that the value obtained from the monthly sampling strategy was approximately double that obtained with the daily sampling strategy when the detritus flux was relatively large, particularly in March and October. Nonetheless, our limited efforts reveal that CH₄ emissions altogether led to as little as ~2.8% of the C uptake via F_{CO2} on a C balance basis and thus allow us to infer the significance of hydrologic flows in leaching C from coastal wetlands.

Abbreviations

GPP: Gross primary production; NPP: Net primary productivity; ANPP: Above-ground net primary production; BNPP: Belowground net primary production; EC: Eddy covariance; MODIS: Moderate-resolution imaging spectrometer; GPP_{EC}: GPP based on situ eddy covariance flux towers; GPP_{MODIS}: GPP based on MODIS time series; ΔGPP: The Difference between GPP_{EC} and GPP_{MODIS}; DOC: Dissolved organic carbon; DIC: Dissolved inorganic carbon; POC: Particulate organic carbon; GEE: Gross ecosystem exchange; NEE: Net ecosystem exchange; NEP: Net ecosystem production; C: Carbon; CN: Carbon/nitrogen; F_{CO2}: Net ecosystem exchanges of CO₂; F_{CH4}: Net ecosystem exchanges of CH₄; ER: Ecosystem respiration; PPFD: Photosynthetic photon flux density; LAI: Leaf area index; FPAR: The Fraction of photosynthetically active radiation; FAPAR: The Fraction of absorbed photosynthetically active radiation; T: Temperature; SM: Soil moisture; VPD: Water vapor pressure deficit; NDVI: Normalized difference vegetation index; EVI: Enhanced vegetation index; ε_g: Maximum light-use efficiency.

Supplementary Information

The online version contains supplementary material available at <https://doi.org/10.1186/s13717-021-00340-2>.

Additional file 1: Fig. S1. Frequencies of net daily detrital carbon flux. A positive flux suggests a net loss, and a negative flux indicates a net gain.

Acknowledgements

We would like to thank our student assistants for their help with the fieldwork, particularly Jun Ma and Wanben Wu for downloading and processing the MODIS-based GPP data from the U.S. Geological Survey. We thank Ying Huang, Zutao Ouyang, Sikai Wang, Chao Song, Tao Zhang and Gang Yang for the constructive revisions that improved a first version of the manuscript. Appreciation is extended to the US-China Carbon Consortium (USCCC). The first author is also grateful to the China Scholarship Council (CSC) for providing a scholarship at the University of Texas at Austin (UT-Austin). We also thank Kristine Blakeslee for editing the manuscript. Thanks are extended to two anonymous referees for their constructive suggestions and fruitful comments.

Authors' contributions

BZ and YG designed this study. YG and JC conceived the ideas. TZ, HG and YG set up the field experiment and collected the data. YG performed the statistical analyses and graphs. BZ, PZ and FZ provided support for the sampling and laboratory analyses. JC and SM contributed to the interpretation and discussion of the results. YG and TZ led the writing of the manuscript, and all other authors contributed to the revision and discussion of the results. All authors read and approved the final manuscript.

Funding

This work was supported by the Open Research Fund of the State Key Laboratory of Estuarine and Coastal Research (Grant No. SKLEC-KF201912), the Foundation of Key Laboratory of Yangtze River Water Environment, Ministry of Education (Tongji University), China, (Grant No. YRWEF202105), the Natural Science Fund of Shanghai (Grant No. 19ZR1470300), the Natural Science Foundation of China (Grant No. 32071584), the Special Fund for Natural Resources Development of Jiangsu Province (Marine Science and Technology Innovation) (Grant No. JSZRHYKJ202109) and the Central Public-interest Scientific Institution Basal Research Fund, ECSFR, CAFS (Grant No. 2021M04).

Availability of data and materials

The datasets used during the current study are available from the corresponding author upon reasonable request.

Declarations

Ethics approval and consent to participate

Not applicable.

Consent for publication

Not applicable.

Competing interests

The authors declare that they have no competing interests.

Author details

¹Key Laboratory of East China Sea & Oceanic Fishery Resources Exploitation and Utilization, Scientific Observing and Experimental Station of Fisheries Resources and Environment of East China Sea and Yangtze Estuary, East China Sea Fisheries Research Institute, Chinese Academy of Fishery Sciences, Shanghai 200090, China. ²Ministry of Education Key Laboratory for Biodiversity Science and Ecological Engineering, Coastal Ecosystems Research Station of the Yangtze River Estuary, and Institute of Eco-Chongming (IEC), Fudan University, Shanghai 200438, China. ³Department of Geological Sciences, University of Texas at Austin, Austin, TX 78712, USA. ⁴Department of Geography and Center for Global Change and Earth Observations (CGCEO), Michigan State University, East Lansing, MI 48824, USA. ⁵Eastern Forest Environmental Threat Assessment Center, Southern Research Station, USDA Forest Service, Research Triangle Park, NC 27709, USA.

Received: 3 August 2021 Accepted: 28 October 2021

Published online: 29 November 2021

References

- Abdul-Aziz Ol, Ishtiaq KS, Tang J, Moseman-Valtierra S, Kroeger KD, Gonneea ME et al (2018) Environmental controls, emergent scaling, and predictions of greenhouse gas (GHG) fluxes in coastal salt marshes. *J Geophys Res-Biogeosci* 123(7):2234–2256. <https://doi.org/10.1029/2018JG004556>
- Aguilón M, Mitra B, Noormets A, Minick K, Prajapati P, Gavazzi M et al (2020) Long-term carbon flux and balance in managed and natural coastal forested wetlands of the Southeastern USA. *Agr Forest Meteorol* 288–289:108022. <https://doi.org/10.1016/j.agrformet.2020.108022>
- Alongi DM (2014) Carbon cycling and storage in mangrove forests. *Annu Rev Mar Sci* 6:195–219. <https://doi.org/10.1146/annurev-marine-010213-135020>
- Aufdenkampe AK, Mayorga E, Raymond PA, Melack JM, Doney SC, Alin SR et al (2011) Riverine coupling of biogeochemical cycles between land, oceans, and atmosphere. *Front Ecol Environ* 9(1):53–60. <https://doi.org/10.1890/100014>
- Bouchard V (2007) Export of organic matter from a coastal freshwater wetland to Lake Erie: an extension of the outwelling hypothesis. *Aquat Ecol* 41(1):1–7. <https://doi.org/10.1007/s10452-006-9044-4>
- Bouchard V, Creach V, Lefeuve JC, Bertru G, Mariotti A (1998) Fate of plant detritus in a European salt marsh dominated by *Atriplex portulacoides* (L.) Aellen. *Hydrobiologia* 373–374:75–87. <https://doi.org/10.1023/A:1017026430513>
- Call M, Sanders CJ, Macklin PA, Santos IR, Maher DT (2019) Carbon outwelling and emissions from two contrasting mangrove creeks during the monsoon storm season in Palau, Micronesia. *Estuar Coast Shelf S* 218:340–348. <https://doi.org/10.1016/j.ecss.2019.01.002>
- Chen NW, Krom MD, Wu YQ, Yu D, Hong HS (2018) Storm induced estuarine turbidity maxima and controls on nutrient fluxes across river-estuary-coast continuum. *Sci Total Environ* 628–629:1108–1120. <https://doi.org/10.1016/j.scitotenv.2018.02.060>
- Chu H, Chen J, Gottgens J, Ouyang Z, John R, Czajkowski KP et al (2014) Net ecosystem CH₄ and CO₂ exchanges in a Lake Erie coastal marsh and a nearby cropland. *J Geophys Res-Biogeosci* 119:722–740. <https://doi.org/10.1002/2013JG002520>
- Chung CH (2006) Forty years of ecological engineering with *Spartina* plantations in China. *Ecol Eng* 27(1):49–57. <https://doi.org/10.1016/j.ecoleng.2005.09.012>
- Coch C, Lamoureux SF, Knoblauch C, Eischeid I, Fritz M, Obu J et al (2018) Summer rainfall dissolved organic carbon, solute, and sediment fluxes in a small Arctic coastal catchment on Herschel Island (Yukon Territory, Canada). *Arct Sci* 4(4):750–780. <https://doi.org/10.1139/as-2018-0010>
- Cole JJ, Prairie YT, Caraco NF, McDowell WH, Tranvik LJ, Striegl RG et al (2007) Plumbing the global carbon cycle: Integrating inland waters into the terrestrial carbon budget. *Ecosystems* 10(1):172–185. <https://doi.org/10.1007/s10021-006-9013-8>
- Couwenberg J, Thiele A, Tanneberger F, Augustin J, Bärtsch S, Dubovik D et al (2011) Assessing greenhouse gas emissions from peatlands using vegetation as a proxy. *Hydrobiologia* 674(1):67–89. <https://doi.org/10.1007/s10750-011-0729-x>
- Cui W, Chui TFM (2019) Temporal and spatial variations of energy balance closure across FLUXNET research sites. *Agr Forest Meteorol* 271:12–21. <https://doi.org/10.1016/j.agrformet.2019.02.026>
- Dame RT, Chrzanowski T, Bildstein K, Kjerfve B, Mckellar H, Nelson D et al (1986) The outwelling hypothesis and North Inlet, South Carolina. *Mar Ecol Prog Ser* 33(3):217–229. <https://doi.org/10.3354/meps033217>
- Dankers N, Binsbergen M, Zegers K (1984) Transportation of water, particulate and dissolved organic and inorganic matter between a salt marsh and Ems-Dollard estuary, the Netherlands. *Estuar Coast Shelf S* 19(2):143–165. [https://doi.org/10.1016/0272-7714\(84\)90061-1](https://doi.org/10.1016/0272-7714(84)90061-1)
- Das A, Justic D, Swenson E, Turner RE, Inoue M, Park D (2011) Coastal land loss and hypoxia: the “outwelling” hypothesis revisited. *Environ Res Lett* 6(2):025001. <https://doi.org/10.1088/1748-9326/6/2/025001>
- Detto M, Verfaillie J, Anderson F, Xu L, Baldocchi D (2011) Comparing laser-based open- and closed-path gas analyzers to measure methane fluxes using the eddy covariance method. *Agr Forest Meteorol* 151:1312–1324. <https://doi.org/10.1016/j.agrformet.2011.05.014>
- Dhillon GS, Inamdar S (2014) Storm event patterns of particulate organic carbon (POC) for large storms and differences with dissolved organic carbon (DOC). *Biogeochemistry* 118(1):61–81. <https://doi.org/10.1007/s10533-013-9905-6>
- Dinsmore KJ, Billett MF, Skiba UM, Rees RM, Drewer J, Helfter C (2010) Role of the aquatic pathway in the carbon and greenhouse gas budgets of a peatland catchment. *Glob Change Biol* 16(10):2750–2762. <https://doi.org/10.1111/j.1365-2486.2009.02119.x>
- Drake TW, Raymond PA, Spencer RGM (2018) Terrestrial carbon inputs to inland waters: a current synthesis of estimates and uncertainty. *Limnol Oceanogr Lett* 3(3):132–142. <https://doi.org/10.1002/lol2.10055>
- Duarte B, Valentim JM, Dias JM, Silva H, Marques JC, Caçador I (2014) Modeling sea level rise (SLR) impacts on salt marsh detrital outwelling C and N exports from an estuarine coastal lagoon to the ocean (Ria de Aveiro, Portugal). *Ecol Model* 289:36–44. <https://doi.org/10.1016/j.ecolmodel.2014.06.020>
- Duarte B, Vaz N, Valentim J, Dias JM, Silva H, Marques JC et al (2017) Revisiting the outwelling hypothesis: modelling salt marsh detrital metal exports under extreme climatic events. *Mar Chem* 191:24–33. <https://doi.org/10.1016/j.marchem.2016.12.002>
- Evans CD, Thomas DN (2016) Controls on the processing and fate of terrestrially-derived organic carbon in aquatic ecosystems: synthesis of special issue. *Aquat Sci* 78(3):1–4. <https://doi.org/10.1007/s00027-016-0470-7>
- Fagherazzi S, Wiberg PL, Temmerman S, Struyf E, Zhao Y, Raymond PA (2013) Fluxes of water, sediments, and biogeochemical compounds in salt marshes. *Ecol Process* 2:3. <https://doi.org/10.1186/2192-1709-2-3>
- Ganju NK, Defne Z, Elsey-Quirk T, Moriarty JM (2019) Role of tidal wetland stability in lateral fluxes of particulate organic matter and carbon. *J Geophys Res-Biogeosci* 124(5):1265–1277. <https://doi.org/10.1029/2018JG004920>
- Gao JH, Zhen XF, Lian C, Wang YP, Bai F, Li J (2016) The effect of biomass variations of *Spartina alterniflora* on the organic carbon content and composition of a salt marsh in northern Jiangsu Province, China. *Ecol Eng* 95:160–170. <https://doi.org/10.1016/j.ecoleng.2016.06.088>
- Gao Y, Ouyang Z, Shao C, Chu H, Su Y, Guo H et al (2018) Field observation of lateral detritus carbon flux in a coastal wetland. *Wetlands* 38(3):613–625. <https://doi.org/10.1007/s13157-018-1005-x>
- Gao Y, Peng R, Ouyang Z, Shao C, Chen J, Zhang T et al (2020) Enhanced lateral exchange of carbon and nitrogen in a coastal wetland with invasive *Spartina alterniflora*. *J Geophys Res-Biogeosci* 125(5):e2019JG005459. <https://doi.org/10.1029/2019JG005459>
- Gounand I, Harvey E, Little CJ, Altermatt F (2017) Meta-ecosystems 2.0: rooting the theory into the field. *Trends Ecol Evol* 33(1):36–46. <https://doi.org/10.1016/j.tree.2017.10.006>
- Gounand I, Little CJ, Harvey E, Altermatt F (2018) Cross-ecosystem carbon flows connecting ecosystems worldwide. *Nat Commun* 9(1):4825. <https://doi.org/10.1038/s41467-018-07238-2>
- Grachev AA, Fairall CW, Blomquist BW, Fernando HJS, McCaffrey KL (2020) On the surface energy balance closure at different temporal scales. *Agr Forest Meteorol* 281:107823. <https://doi.org/10.1016/j.agrformet.2019.107823>

- Gravel D, Guichard F, Loreau M, Mouquet N (2010) Source and sink dynamics in meta-ecosystems. *Ecology* 91(7):2172–2184. <https://doi.org/10.1890/09-0843.1>
- Guo HQ, Noormets A, Zhao B, Chen JQ, Sun G, Gu YJ et al (2009) Tidal effects on net ecosystem exchange of carbon in an estuarine wetland. *Agr Forest Meteorol* 149:1820–1828. <https://doi.org/10.1016/j.agrformet.2009.06.010>
- Harishma KM, Sandeep S, Sreekumar VB (2020) Biomass and carbon stocks in mangrove ecosystems of Kerala, southwest coast of India. *Ecol Process* 9:31. <https://doi.org/10.1186/s13717-020-00227-8>
- Hemminga MA, Cattrijsse A, Wielemaker A (1996) Bedload and nearbed detritus transport in a tidal saltmarsh creek. *Estuar Coast Shelf S* 42(1):55–62. <https://doi.org/10.1006/ecss.1996.0005>
- Holden J, Smart RP, Dinsmore KJ, Baird AJ, Billett MF, Chapman PJ (2012) Natural pipes in blanket peatlands: major point sources for the release of carbon to the aquatic system. *Glob Change Biol* 18(12):3568–3580. <https://doi.org/10.1111/gcb.12004>
- Huang Y, Guo H, Chen X, Chen Z, van der Tol C, Zhou Y et al (2019) Meteorological controls on evapotranspiration over a coastal salt marsh ecosystem under tidal influence. *Agr Forest Meteorol* 279:107755. <https://doi.org/10.1016/j.agrformet.2019.107755>
- Huang Y, Chen Z, Tian B, Zhou C, Wang J, Ge Z et al (2020) Tidal effects on ecosystem CO₂ exchange in a *Phragmites* salt marsh of an intertidal shoal. *Agr Forest Meteorol* 292–293:108108. <https://doi.org/10.1016/j.agrformet.2020.108108>
- Hunsinger GB, Mitra S, Findlay SEG, Fischer DT (2010) Wetland-driven shifts in suspended particulate organic matter composition of the Hudson River estuary, New York. *Limnol Oceanogr* 55(4):1653–1667. <https://doi.org/10.4319/lo.2010.55.4.1653>
- Jenerette GD, Lal R (2005) Hydrologic sources of carbon cycling uncertainty throughout the terrestrial-aquatic continuum. *Glob Change Biol* 11(11):1873–1882. <https://doi.org/10.1111/j.1365-2486.2005.01021.x>
- Law BE, Anthoni PM, Aber JD (2000) Measurements of gross and net ecosystem productivity and water vapour exchange of a *Pinus ponderosa* ecosystem, and an evaluation of two generalized models. *Glob Change Biol* 6(2):155–168. <https://doi.org/10.1046/j.1365-2486.2000.00291.x>
- Lehman PW, Mayr S, Liu L, Tang A (2015) Tidal day organic and inorganic material flux of ponds in the Liberty Island freshwater tidal wetland. *SpringerPlus* 4(1):273. <https://doi.org/10.1186/s40064-015-1068-6>
- Li H, Dai S, Ouyang Z, Xiao X, Guo H, Gu C et al (2018) Multi-scale temporal variation of methane flux and its controls in a subtropical tidal salt marsh in eastern China. *Biogeochemistry* 137(1–2):163–179. <https://doi.org/10.1007/s10533-017-0413-y>
- Liao CZ, Luo YQ, Jiang LF, Zhou XH, Wu XW, Fang CM et al (2007) Invasion of *Spartina alterniflora* enhanced ecosystem carbon and nitrogen stocks in the Yangtze Estuary, China. *Ecosystems* 10(8):1351–1361. <https://doi.org/10.1007/s10021-007-9103-2>
- Lomnicki A, Bandola E, Jankowska K (1968) Modification of the Wiegert-Evans method for estimation of net primary production. *Ecology* 49(1):147–149. <https://doi.org/10.2307/1933570>
- Loreau M, Mouquet N, Holt RD (2003) Meta-ecosystems: a theoretical framework for a spatial ecosystem ecology. *Ecol Lett* 6(8):673–679. <https://doi.org/10.1046/j.1461-0248.2003.00483.x>
- Maxwell TM, Silva LCR (2020) A state factor model for ecosystem carbon-water relations. *Trends Plant Sci* 25(7):652–660. <https://doi.org/10.1016/j.tplan.2020.02.007>
- Mfilinge PL, Meziiane T, Bachok Z, Tsuchiya M (2005) Litter dynamics and particulate organic matter outwelling from a subtropical mangrove in Okinawa Island South Japan. *Estuar Coast Shelf S* 63(1–2):301–313. <https://doi.org/10.1016/j.ecss.2004.11.022>
- Mitra B, Minick K, Miao G, Domec J, Prajapati P, McNulty SG et al (2020) Spectral evidence for substrate availability rather than environmental control of methane emissions from a coastal forested wetland. *Agr Forest Meteorol* 291:108062. <https://doi.org/10.1016/j.agrformet.2020.108062>
- Najjar RG, Herrmann M, Alexander R, Boyer EW, Burdige D, Butman D et al (2018) Carbon budget of tidal wetlands, estuaries, and shelf waters of Eastern North America. *Global Biogeochem Cy* 32(3):389–416. <https://doi.org/10.1002/2017GB005790>
- Odum EP (2000) Tidal marshes as outwelling/pulsing systems. In: Weinstein MP, Kreeger DA (eds) Concepts and controversies in tidal marsh ecology. Kluwer Academic Publishers, Dordrecht, pp 3–7
- Osburn CL, Rudolph JC, Paerl HW, Hounshell AG, Van Dam BR (2019) Lingering carbon cycle effects of hurricane Matthew in North Carolina's coastal waters. *Geophys Res Lett* 46(5):2654–2661. <https://doi.org/10.1029/2019GL082014>
- Palomo L, Niell FX (2009) Primary production and nutrient budgets of *Sarcocornia perennis* ssp *alpini* (Lag.) Castroviejo in the salt marsh of the Palmones River estuary (Southern Spain). *Aquat Bot* 91(3):130–136. <https://doi.org/10.1016/j.aquabot.2009.04.002>
- Parker RJ, Boesch H, McNorton J, Comyn-Platt E, Gloor M, Wilson C et al (2018) Evaluating year-to-year anomalies in tropical wetland methane emissions using satellite CH₄ observations. *Remote Sens Environ* 211:261–275. <https://doi.org/10.1016/j.rse.2018.02.011>
- Prasad MBK, Kumar A, Ramanathan AL, Datta DK (2017) Sources and dynamics of sedimentary organic matter in Sundarban mangrove estuary from Indo-Gangetic delta. *Ecol Process* 6:8. <https://doi.org/10.1186/s13717-017-0076-6>
- Prince SD, Goward SN (1995) Global primary production: a remote sensing approach. *J Biogeogr* 22(4/5):815–835. <https://doi.org/10.2307/2845983>
- Rahaman SMB, Sarder L, Rahaman MS, Ghosh AK, Biswas SK, Siraj SS et al (2013) Nutrient dynamics in the Sundarbans mangrove estuarine system of Bangladesh under different weather and tidal cycles. *Ecol Process* 2:29. <https://doi.org/10.1186/2192-1709-2-29>
- Reichstein M, Falge E, Baldocchi D, Papale D, Aubinet M, Berbigier P et al (2005) On the separation of net ecosystem exchange into assimilation and ecosystem respiration: review and improved algorithm. *Glob Change Biol* 11(9):1424–1439. <https://doi.org/10.1111/j.1365-2486.2005.001002.x>
- Ridd P, Sandstrom MW, Wolanski E (1988) Outwelling from tropical tidal salt flats. *Estuar Coast Shelf S* 26(3):243–253. [https://doi.org/10.1016/0272-7714\(88\)90063-7](https://doi.org/10.1016/0272-7714(88)90063-7)
- Rogers K, Kelleway JJ, Saintilan N, Megonigal JP, Adams JB, Holmquist JR et al (2019) Wetland carbon storage controlled by millennial-scale variation in relative sea-level rise. *Nature* 567(7746):91–95. <https://doi.org/10.1038/s41586-019-0951-7>
- Ruimy A, Saugier B, Dedieu G (1994) Methodology for the estimation of terrestrial net primary production from remotely sensed data. *J Geophys Res-Atmos* 99(D3):5263–5283. <https://doi.org/10.1029/93JD03221>
- Running SW, Nemani RR, Ann HF, Zhao M, Matt R, Hirofumi H (2004) A continuous satellite-derived measure of global terrestrial primary production. *Bioscience* 54(6):547–560. [https://doi.org/10.1641/0006-3568\(2004\)054\[0547:ACSMOG\]2.0.CO;2](https://doi.org/10.1641/0006-3568(2004)054[0547:ACSMOG]2.0.CO;2)
- Running S, Zhao M (2019) MOD17A2HGF MODIS/Terra gross primary productivity gap-filled 8-day L4 global 500 m SIN grid v006. NASA EOSDIS Land Processes DAAC. <https://doi.org/10.5067/MODIS/MOD17A2HGF.006>. Accessed 7 Jul 2020.
- Santos IR, Maher DT, Larkin R, Webb JR, Sanders CJ (2019) Carbon outwelling and outgassing vs. burial in an estuarine tidal creek surrounded by mangrove and saltmarsh wetlands. *Limnol Oceanogr* 64:996–1013. <https://doi.org/10.1002/lno.11090>
- Schindler DE, Smits AP (2017) Subsidies of aquatic resources in terrestrial ecosystems. *Ecosystems* 20(1):78–93. <https://doi.org/10.1007/s10021-016-0050-7>
- Sippo JZ, Maher DT, Schulz KG, Sanders CJ, McMahon A, Tucker J et al (2019) Carbon outwelling across the shelf following a massive mangrove die-back in Australia: insights from radium isotopes. *Geochim Cosmochim Acta* 253:142–158. <https://doi.org/10.1016/j.gca.2019.03.003>
- Sitters J, Atkinson CL, Guelzow N, Kelly P, Sullivan LL (2015) Spatial stoichiometry: cross-ecosystem material flows and their impact on recipient ecosystems and organisms. *Oikos* 124(7):920–930. <https://doi.org/10.1111/oik.02392>
- Soininen J, Bartels P, Heino J, Luoto M, Hillebrand H (2015) Toward more integrated ecosystem research in aquatic and terrestrial environments. *Bioscience* 65(2):174–182. <https://doi.org/10.1093/biosci/biu216>
- Sousa AI, Santos DB, Silva EFD, Sousa LP, Cleary DFR, Soares AMVM et al (2017) “Blue carbon” and nutrient stocks of salt marshes at a temperate coastal lagoon (Ria de Aveiro, Portugal). *Sci Rep* 7:41225. <https://doi.org/10.1038/srep41225>

- Swain ED, Krohn D, Langtimm CA (2015) Numerical computation of hurricane effects on historic coastal hydrology in Southern Florida. *Ecol Process* 4:4. <https://doi.org/10.1186/s13717-014-0028-3>
- Taillardat P, Ziegler AD, Friess DA, Widory D, David F, Ohte N et al (2019) Assessing nutrient dynamics in mangrove porewater and adjacent tidal creek using nitrate dual-stable isotopes: a new approach to challenge the Outwelling Hypothesis? *Mar Chem* 214:103662. <https://doi.org/10.1016/j.marchem.2019.103662>
- Tank SE, Fellman JB, Hood E, Kratzberg ES (2018) Beyond respiration: controls on lateral carbon fluxes across the terrestrial-aquatic interface. *Limnol Oceanogr Lett* 3(3):76–88. <https://doi.org/10.1002/lol2.10065>
- Teal JM (1962) Energy flow in the salt marsh ecosystem of Georgia. *Ecology* 43(4):614–624. <https://doi.org/10.2307/1933451>
- Tranvik LJ, Downing JA, Cotner JB, Loiselle SA, Striegl RG, Ballatore TJ et al (2009) Lakes and reservoirs as regulators of carbon cycling and climate. *Limnol Oceanogr* 54(6):2298–2314. https://doi.org/10.4319/lo.2009.54.6_part_2.2298
- Wang X, Ma H, Li R, Song Z, Wu J (2012) Seasonal fluxes and source variation of organic carbon transported by two major Chinese rivers: the Yellow River and Changjiang (Yangtze) River. *Global Biogeochem Cy* 26:GB2025. <https://doi.org/10.1029/2011GB004130>
- Winter P, Schlacher TA, Baird D (1996) Carbon flux between an estuary and the ocean: a case for outwelling. *Hydrobiologia* 337(1–3):123–132. <https://doi.org/10.1007/BF00028513>
- Wolanski E (2016) Bounded and unbounded boundaries - untangling mechanisms for estuarine-marine ecological connectivity: scales of m to 10,000 km—a review. *Estuar Coast Shelf S* 198:378–392. <https://doi.org/10.1016/j.ecss.2016.06.022>
- Wolff WJ, VanEeden MN, Lammens E (1979) Primary production and import of particulate organic matter on a salt marsh in the Netherlands. *Neth J Sea Res* 13(2):242–255. [https://doi.org/10.1016/0077-7579\(79\)90005-X](https://doi.org/10.1016/0077-7579(79)90005-X)
- Wu Y, Bao H, Yu H, Zhang J, Kattner G (2015) Temporal variability of particulate organic carbon in the lower Changjiang (Yangtze River) in the post-Three Gorges Dam period: links to anthropogenic and climate impacts. *J Geophys Res-Biogeosci* 120(11):2194–2211. <https://doi.org/10.1002/2015JG002927>
- Xiao X, Zhang Q, Braswell B, Urbanski S, Boles S, Wofsy S et al (2004) Modeling gross primary production of temperate deciduous broadleaf forest using satellite images and climate data. *Remote Sens Environ* 91(2):256–270. <https://doi.org/10.1016/j.rse.2004.03.010>
- Yan Y, Zhao B, Chen JQ, Guo HQ, Gu YJ, Wu QH et al (2008) Closing the carbon budget of estuarine wetlands with tower-based measurements and MODIS time series. *Glob Change Biol* 14(7):1690–1702. <https://doi.org/10.1111/j.1365-2486.2008.01589.x>
- Yang SL (1999) Sedimentation on a growing intertidal island in the Yangtze River mouth. *Estuar Coast Shelf S* 49(3):401–410. <https://doi.org/10.1006/ecss.1999.0501>
- Yang W, Qiao Y, Li N, Zhao H, Yang R, Leng X et al (2017) Seawall construction alters soil carbon and nitrogen dynamics and soil microbial biomass in an invasive *Spartina alterniflora* salt marsh in eastern China. *Appl Soil Ecol* 110:1–11. <https://doi.org/10.1016/j.apsoil.2016.11.007>
- Yuan W, Cai W, Xia J, Chen J, Liu S, Dong W et al (2014) Global comparison of light use efficiency models for simulating terrestrial vegetation gross primary production based on the LaThuile database. *Agr Forest Meteorol* 192–193:108–120. <https://doi.org/10.1016/j.agrformet.2014.03.007>
- Zhao B, Guo H, Yan Y, Wang Q, Li B (2008) A simple waterline approach for tide-lands using multi-temporal satellite images: a case study in the Yangtze Delta. *Estuar Coast Shelf S* 77(1):134–142. <https://doi.org/10.1016/j.ecss.2007.09.022>
- Zhao B, Yan Y, Guo HQ, He MM, Gu YJ, Li B (2009) Monitoring rapid vegetation succession in estuarine wetland using time series MODIS-based indicators: an application in the Yangtze River Delta area. *Ecol Indic* 9(2):346–356. <https://doi.org/10.1016/j.ecolind.2008.05.009>

Publisher's Note

Springer Nature remains neutral with regard to jurisdictional claims in published maps and institutional affiliations.

Submit your manuscript to a SpringerOpen[®] journal and benefit from:

- Convenient online submission
- Rigorous peer review
- Open access: articles freely available online
- High visibility within the field
- Retaining the copyright to your article

Submit your next manuscript at ► [springeropen.com](https://www.springeropen.com)